


# Bromelain Kinetics and Mechanism on Myofibril from Golden Pomfret (*Trachinotus blochii*)

Xiao Feng, Shasha Hang, Yige Zhou, Qin Liu, and Hongshun Yang 

**Abstract:** Bromelain was used to tenderize golden pomfrets (*Trachinotus blochii*). The enzyme kinetic model was  $x = 2.447 \times \ln[1 + (1332.21 \times \frac{E_0}{S_0} - 1.74)t]$ , which indicated that the degree of hydrolysis (DH,  $x$ ) was dependent on hydrolysis time ( $t$ ), the initial concentration of myofibril ( $S_0$ ) and bromelain ( $E_0$ ). The relationship between the overall hydrolysis rate ( $v$ ),  $S_0$ ,  $E_0$ , and  $t$  is demonstrated as:  $v = (16.50(\frac{E_0}{S_0}) - 1.33)S_0 \exp\{-2.447 \ln[1 + (1332.21 \frac{E_0}{S_0} - 1.74)t^2]\}$ . Sample of 0.40%  $E_0/S_0$  was further used to study the effects of hydrolysis time on the changes of proteins, peptides, free amino acids (FAA), and protein nanostructure. SDS-PAGE result showed that myosin heavy chain was degraded dramatically from 22.88% before treatment to 12.03% after 2 min bromelain treatment. Meanwhile, bromelain did not exhibit activity towards actin, trypomyosin, myosin light chain, and troponin C. A general increase of amino acids indicated the increased DH and the preferential cleavage sites of bromelain in the descending order of lysine, glutamic acid, glycine, ornithine, methionine sulfoxide, and alanine. Atomic force microscope images showed that the strip-like structure of myofibril was considerably degraded by bromelain, and the granulation of protein after 20 min indicated possible self-assembling of protein hydrolysate. Confocal laser scanning microscopy further confirmed the degradation of myofibril proteins and formation of protein aggregates.

**Keywords:** atomic force microscope, amino acid, modeling, myofibril, protease

**Practical Application:** Meat of golden pomfrets is tough, thus not idea for fish balls or fish cakes. Tenderization is essential to achieve desired texture and consumer acceptance, especially for this fish meat with intrinsic hard texture. Bromelain can be extracted from pineapple processing waste. Enzymatic kinetics was studied to instruct industry to control the tenderness of the processed fish meat. The microstructural and mechanism study elucidate the process, thus could be applied to improve the quality of the seafood products correspondingly.

## Introduction

Fish is rich in proteins and tasty, and fishery products are popular worldwide. In Singapore, fishery products, such as fish balls, are highly demanded and favored in market. It has been reported that over 90% local food consumption relies on the imported supplies, and only 8% fish is farmed locally, which leads to food security issues. To raise self-sufficiency level in Singapore, golden pomfret (*Trachinotus blochii*, GP) was spawned locally.

Texture and tenderness are recognized as highly valued consumer attributes (Lonergan, Zhang, & Lonergan, 2010). Although GP is expected to boost local fish supply in the next few years, it is not yet commercialized for fishery product manufacture due to the intrinsic hard texture. Myofibrils are the main components of muscle fibers, and account for 60% to 80% of the total proteins in fish (Delbarre-Ladrat, Chéret, Taylor, & Verrez-Bagnis, 2006). Evidence shows that the length and width of myofibrils are related to the texture and tenderness of fish muscle, although changes of the myofibril nanostructure have significant effects on the texture

of fishery products (Feng, Fu, & Yang, 2017a; Lobo, Ventanas, Morcuende, & Estévez, 2016).

Plant enzymes have shown strong proteolytic effects towards meat tenderization, such as papain, ficin and bromelain (Delbarre-Ladrat et al., 2006; Gerelt, Ikeuchi, & Suzuki, 2000). Bromelain, a cysteine proteinase, has demonstrated to tenderize meat with juicier texture, higher water holding capacity and improved flavors (Esti, Benucci, Liburdi, & Garzillo, 2015; Kim & Taub, 1991). Previous studies have exploited the applications of bromelain to process fishery products and improve their qualities (Feng, Zhu, Liu, & Yang, 2017c). For example, tilapia and India carps were successfully hydrolyzed by the treatment of bromelain, and beneficial peptides were generated to increase their nutritional values (Klompong, Benjakul, Kantachote, & Shahidi, 2007). The loach and round scads were hydrolyzed by bromelain to generate fish protein hydrolysates with improved quality and functionality (Thiansilakul, Benjakul, & Shahidi, 2007). Enzyme hydrolysis kinetics were also studied. For example, a quadratic model were used to examine the effects of degree of hydrolysis (DH) on the functional properties of the salmon waste (Gbogouri, Linder, Fanni, & Parmentier, 2004). Michaelis–Menten equation was applied to describe the microbial enzyme hydrolysis on the fish substrates (Rebeca, Pena-Vera, & Diaz-Castaneda, 1991). The effects of pH and temperature on the hydrolysis rate were investigated in yellow-stripe trevally and fish frames, and it was found that the DH had linear relationship with the log concentration of the enzyme (Himonides, Taylor, & Morris, 2011; Klompong et al., 2007).

JFDS-2018-0146 Submitted 2/4/2018, Accepted 5/13/2018. Authors Feng, Hang, Zhou, Liu, and Yang are with Food Science and Technology Programme, c/o Dept. of Chemistry, Natl. Univ. of Singapore, Singapore, 117543, Singapore. Authors Feng, Hang, Zhou, Liu, and Yang are also with Natl. Univ. of Singapore (Suzhou) Research Inst., 377 Lin Quan Street, Suzhou Industrial Park, Suzhou, Jiangsu, 215123, P.R. China. Author Hang is also with Fujian Putian Sea-100 Food Co., Ltd., Putian, Fujian, 355100, P.R. China. Direct inquiries to author Yang (E-mail: chmynghs@nus.edu.sg).

Our previous study applied bromelain to tenderize GP, which was used to manufacture fish balls with acceptable texture and flavor. In the process of enzyme hydrolysis, proteins were hydrolyzed to different peptides and subfragments, which potentially improved the nutritious values and tenderness of fishery products (Feng et al., 2017c). However, further studies, such as the enzyme kinetics and mechanism, are not investigated and elaborated.

The objective of this research was to further understand the enzyme kinetics and mechanism of bromelain on GP. The effects of enzyme concentration and substrate concentration on the DH and the overall hydrolytic rate were examined to investigate the enzyme kinetics and build the kinetic models. The compositional changes of myofibrils and FAA generation were analyzed to understand the enzyme mechanism of bromelain on the fish muscle. The nanostructural changes of myofibril during hydrolysis were measured by AFM and CLSM.

## Materials and Methods

### Myofibril protein extraction and enzymatic hydrolysis

#### Extraction of myofibrils from golden pomfret (MGP).

Commercial local GP, sized 500 to 700 g, was purchased from a nearby local supermarket (NTUC Fairprice Co-Operative, Singapore). GPs were stored in a cold storage bag and transferred to the lab within 30 min to maintain the freshness. The head, fins, skin and bones of GP were removed completely. Fillets picked from the dorsal region of the fish and were minced into smaller pieces, and then homogenized with a blender.

MGP were extracted from prepared flesh samples using the method described by previous reports with modifications (Feng, Bansal, & Yang, 2016; Liu & Xiong, 2015). Instead of walk-in cooler, ice-water bath was used to control the temperature during the MGP extraction. The supernatant containing myofibril extract was kept under  $-20\text{ }^{\circ}\text{C}$  for further experiments.

**Enzymatic hydrolysis by bromelain.** Before bromelain hydrolysis, the concentration of proteins in myofibril was measured following Bradford method (Bradford, 1976). Extracted myofibril of 200 mL was hydrolyzed by 0.40% (bromelain–myofibril ratio, w/w) commercial bromelain powder (50,000 U/g, Hebei Baiwei Biotechnology Co. Ltd., Handan, Hebei, China) with constant stirring at 300 rpm for 30 min under  $0\text{ }^{\circ}\text{C}$ , pH 6.8. During hydrolysis process, 2 mL hydrolyzed samples before and after 0.5, 2, 4, 6, 8, 10, 15, 20, 25, and 30 min treatment were pipetted into tubes, and quenched by heating in  $100\text{ }^{\circ}\text{C}$  water bath for 5 min (Ahern & Klivanov, 1985). The hydrolyzed myofibril samples were centrifuged to remove the precipitates and then stored under  $-20\text{ }^{\circ}\text{C}$  for future analysis (Suwal, Ketnawa, Huang, & Liceaga, 2017).

### Determination of amino nitrogen and DH

Myofibrillar protein extracts with three concentrations were prepared, and were treated with different bromelain–myofibril ratio (w/w) varying from 0.05% to 0.97%. All the 10 batches were hydrolyzed for 30 min under the same conditions ( $0\text{ }^{\circ}\text{C}$ , pH 6.8). The DH was based on the concentration of amino nitrogen, which was determined through formaldehyde titration assay with slightly modifications (Xu, Yu, Xue, Xue, & Ren, 2008). Phenolphthalein ethanol solution (0.5%, w/v) was used as indicator. Formaldehyde solution (37%, v/v) was neutralized (pH 7) by 0.02 mol/L sodium hydroxide, and sodium hydroxide (0.001 mol/L) was used for titration.

DH was calculated from the equation below:

$$\text{DH}(\%) = \frac{\text{formaldehyde nitrogen content}}{\text{total nitrogen content}} \times 100\% \quad (1)$$

Total nitrogen content is determined by Kjeldahl factor and protein concentration by Bradford protein assay method (Bradford, 1976).

### SDS-PAGE

Myofibrillar proteins were analyzed by one dimensional SDS-PAGE. Bio-Rad protein assay protocol and 4% to 20% gradient gel was used to measure the protein concentration. The volume of each sample was adjusted to make sure the protein content was  $20\text{ }\mu\text{g}$  in every well of the gradient gel. The SDS-PAGE running buffer, sample loading buffer were purchased from Bio-Rad Laboratories, Inc., Hercules, CA, USA. The protein standard (10 to 250 kDa) was used as the marker (Kim et al., 2017). Electrophoresis was performed on a Bio-Rad Mini-PROTEAN Tetra Cell at 80 V for approximately 100 min, followed by gel staining and destaining processes. The experiment was repeated five times for the band intensity quantification (Delles, Xiong, & True, 2011; Mohhtar, Perera, & Quek, 2010). The gel image was captured using the gel imaging system G:BOX EF2 (Syngene, Synoptics Ltd., Cambridge, U.K.) and analyzed using the computer software CLIQS 1D Pro (TotalLab Ltd., Newcastle upon Tyne, U.K.).

### Analysis of FAA

The sample was centrifuged under  $17,000\text{ }g$  for 10 min at  $4\text{ }^{\circ}\text{C}$ . The supernatant was removed by solid phase extraction followed by a derivatization and a liquid-liquid extraction according to the manual from a Phenomenex EZ:faast<sup>TM</sup> Amino Acid Analysis Kit (Torrance, Calif., USA). The eluting medium was freshly prepared before the procedure by mixing elution medium component 1 and elution medium component 2 in the ratio of 3:2 (v/v). Sample of  $50\text{ }\mu\text{L}$  (pH was adjusted among 2 to 5 by 0.5 M HCl) and  $100\text{ }\mu\text{L}$  internal standard were pipetted into a vial and mixed by vortex. The solution was passed through 1.5 mL syringe with sorbent tip by pulling very slowly. Deionized water of  $200\text{ }\mu\text{L}$  was pipetted into the same vial and was slowly passed through the syringe again. The liquid in the syringe was discarded after separating the sorbent tip. Eluting medium ( $200\text{ }\mu\text{L}$ ) was pipetted to wet the sorbent tip. The liquid and the sorbent were ejected into a vial. The above procedure was repeated until the tip was clear without sorbent. The ejected mixture was fully homogenized by vortex for at least 1 min.

Next, the mixture was derivatized and analyzed by HPLC-MS/MS with an EZ : fast AAA LC column of  $250\text{ mm} \times 2.0\text{ mm}$  under  $35\text{ }^{\circ}\text{C}$ . Mobile phase A was 10 mmol/L ammonium formate in water, and mobile phase B was 10 mmol/L formate in methanol. The elution percentage of mobile phase B increased linearly from 68% at 0 min to 83% at 13 min, followed by decreasing to 68% at 13.01 min and keeping at 68% until the end. The injection volume and flow rate were  $5\text{ }\mu\text{L}$  and  $0.1375\text{ mL/min}$ , respectively. The nitrogen gas flow rate was  $10\text{ L/min}$  (Sasaoka, Kishimura, Adachi, & Takagi, 2017; Zarei et al., 2016).

### AFM and CLSM

The myofibril supernatant was diluted twenty times using distilled water and homogenized before AFM analysis. The diluted

sample of 20  $\mu\text{L}$  was pipetted onto a clean mica sheet, with a magnetic disc attaching to it. The sample was air-dried at ambient temperature. TT-AFM (AFM workshop, Signal Hill, CA, U.S.A.) equipped with a Sensaprobe TM190-A-15 tip (Applied Nanos-structures, Mountain View, CA, U.S.A.) was used to analyze the morphology of myofibril (Sow & Yang, 2015).

Rhodamine B was purchased from sigma and dissolve in DMSO to dye the myofibril solution. Sample of 30  $\mu\text{L}$  was pipetted on glass slide and dried for 3 hr. System FLUOVIEW FV1000 4.2.2.9 (Olympus, Tokyo, Japan) was used to image the samples, and the scan size was  $211.761 \times 211.761 \mu\text{m}$  (Razzak, Kim, & Chung, 2016).

### Statistical analysis

All the experiments were conducted in triplicate without specific claim. The results were reported as mean  $\pm$  standard deviation (SD). The data analysis of differences among different groups of samples were performed by ANOVA (significance level,  $p < .05$ ) together with post-hoc Duncan's multiple comparison test with IBM SPSS software Version. 19 (SPSS Inc., Chicago, IL, U.S.A.). For AFM analysis, parallel images ( $\geq 15$ ) for each sample were applied for valid statistical results.

## Results and Discussion

### Enzyme kinetics modelling

The DH of treated samples were calculated according to the amount of amino nitrogen. The hydrolysis process was examined within 30 min and the results were shown in Figure 1. It was obvious that the DH increased significantly after the addition of bromelain, and reached a plateau after certain hydrolysis time. It has been proved that the proteolytic hydrolysis of bromelain in aqueous solution at pH 4 to 8.5 follows first-order reaction kinetics (Arshad et al., 2014). Therefore, under constant pH and temperature, the total rate of hydrolysis is:

$$V = S_0 \frac{dx}{dt} = F(S_0, x) \cdot E \quad (2)$$

In Eq. (2),  $V$  is the overall hydrolysis rate (g/mL/min), and  $E$  is the bromelain concentration (mg/mL), whereas  $x$  (%) is the calculated DH. According to the kinetic mechanism on the denaturation of protease, the rate of hydrolysis can also be reported as (Maresca & Ferrari, 2017):

$$V = a S_0 \exp(-bx) \quad (3)$$

In this equation,  $a$  ( $\text{min}^{-1}$ ) and  $b$  are kinetic parameters. From Eq. (2) and (3), it can be deduced that the rate of hydrolysis  $dx/dt$  decreased exponentially as time increased:

$$\frac{dx}{dt} = a \exp(-bx) \quad (4)$$

Further deduction can be obtained through integrating Eq. (4):

$$x = \frac{1}{b} \ln(1 + abt) \quad (5)$$

The kinetic parameters  $a$  and  $b$  were then acquired through non-linear regression fitting by OriginPro 2016 software (OriginLab Corp., Northampton, MA, U.S.A.).

**The effect of time on DH.** In Figure 1, the DH increased with the hydrolysis time and the initial enzyme concentration, but it decreased as the initial myofibril concentration increased, which agreed well with previous findings (Gbogouri et al., 2004; González-Tello, Camacho, Jurado, Paez, & Guadix, 1994). Basically, the DH increased significantly within 10 min, and slowed down since then and became stable after 15 or 20 min reactions. As the DH became stable, the rate of hydrolysis decreased gradually, which may be caused by the following factors: the concentration of the susceptible sites of peptide bonds decreased; some certain products of hydrolysis may inhibit the enzyme activity; and the denaturation of the enzyme (González-Tello, Camacho, Jurado, Paez, & Guadix, 1994). The increase of the bromelain concentration can significantly improve the combination with the substrate and increase the DH. It was observed from Figure 1A–C that the maximum value of the DH increased as the initial bromelain concentration increased.

The DH obtained under different substrate concentrations and a constant bromelain concentration is shown in Figure 1D–F. The DH was 3.49% ( $E_0$ :  $3.75 \times 10^{-3}$  mg/mL;  $S_0$ : 7.5 mg/mL) whereas it increased to 18.40% as the  $E_0$  increased to  $15 \times 10^{-3}$  mg/mL and  $S_0$  decreased to 1.55 mg/mL. The excessive concentration of myofibril could easily lead to the increased viscosity, accompanied with the decreased spread of bromelain and the decreased water activity, which could result in the inhibition of the hydrolysis reactions and decreased DH (Kirk, Borchert, & Fuglsang, 2002).

**Parameters of kinetic model.** Table 1 showed the values of parameters  $a$  and  $b$  under different conditions, which were fitted by nonlinear regression analysis according to the  $x-t$  hydrolysis curves and Eq. (5). It can be observed that  $a$  values basically increased with the increased enzyme concentration, whereas  $b$  values decreased, as the substrate concentration remained the same. The  $3.75 \times 10^{-3}$  mg/mL enzyme addition to 7.50 mg/mL myofibril was an exception, which may result from the far excess substrate concentration with low bromelain concentration. It was observed that  $a$  values had significant dependence on  $E_0$  and  $S_0$ , whereas  $b$  values varied in the small range between 0.32 and 0.68. Therefore, the parameter  $b$  can be considered as a constant with an average values of 0.445. Values of  $a_m$  were the results of fitting  $b_{\text{constant}}$  of 0.445. Meanwhile, as the  $a_m$  value varied significantly with a value when  $E_0/S_0 = 0.97\%$ , this group was excluded from fitting into this model. Thus, with the mean value of  $b = 0.445$ ,  $a_m$  was calculated from Eq. (5):

$$x = \frac{1}{0.445} \ln(1 + 0.445at) \quad (6)$$

The parameter  $a_m$  was linearly fitted with  $E_0/S_0$  (%) and the correlation coefficient ( $r$ ) was 0.9832:

$$a_m = 16.50 \times (E_0/S_0) - 1.33 \quad (7)$$

To combine Eq. (6) and (7), the kinetic model of MGP hydrolyzed by bromelain with  $E_0/S_0$  ranging from 0.10% to 0.71% (pH 6.8, 0 °C) is

$$x = 2.447 \times \ln \left[ 1 + \left( 1332.21 \times \frac{E_0}{S_0} - 1.74 \right) t \right] \quad (8)$$

Equation (8) indicates that the DH ( $x$ ) is affected by  $E_0$ ,  $S_0$ , and  $t$ . The percentage difference (PD) and root mean square

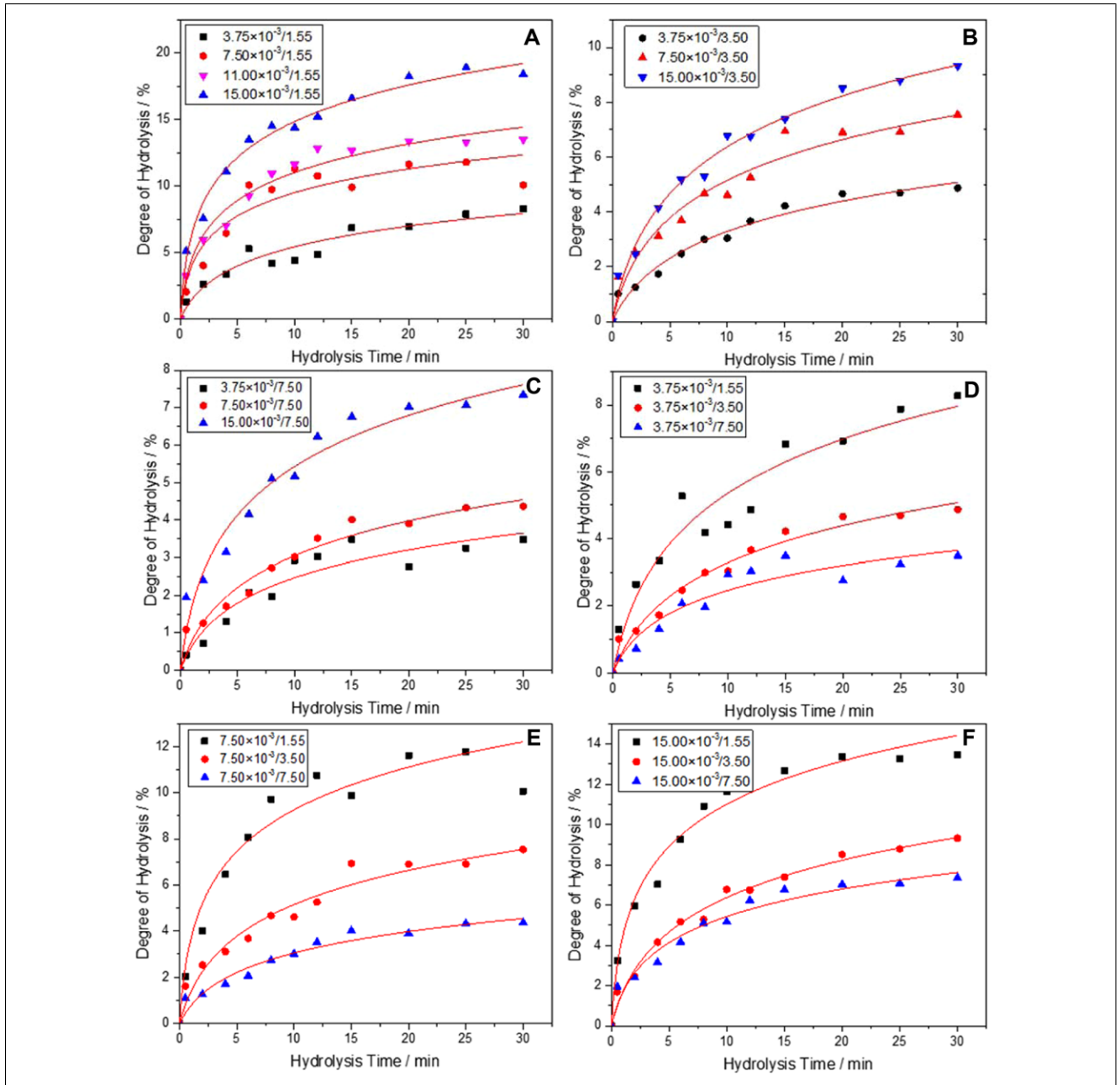


Figure 1—Fitting models of degree of hydrolysis under different  $E_0/S_0$  ratios: treatment with different bromelain and constant myofibril concentration of 1.55 mg/mL (A), 3.50 mg/mL (B), and 7.50 mg/mL (C); treatment with different myofibril concentrations and constant bromelain addition of  $3.75 \times 10^{-3}$  mg/mL (D),  $7.50 \times 10^{-3}$  mg/mL (E), and  $15.0 \times 10^{-3}$  mg/mL (F).

error (RMSE) of this model was calculated as 3.09% and 0.377%, respectively, according to the equations below.

$$RMSE = \sqrt{\frac{(X_{12} - X'_{12})^2 + (X_{20} - X'_{20})^2}{2}} \quad (9)$$

$$PD = \left[ \frac{X_{12} - X'_{12}}{(X_{12} + X'_{12})/2} + \frac{X_{20} - X'_{20}}{(X_{20} + X'_{20})/2} \right] \div 2 \times 100 \quad (10)$$

$X_{12}$  is the DH at 12 min as  $E_0/S_0$  is 0.48%, and  $X'_{12}$  is the predicted DH calculated from Eq. (8).  $X_{20}$  is the DH at 20 min as  $E_0/S_0$  is 0.48%, although  $X'_{20}$  is the predicted DH calculated from

Eq. (8). The low PD and RMSE values indicated the accuracy of this kinetic model to explain the relation among DH,  $E_0$ ,  $S_0$ , and hydrolysis time.

The hydrolysis rate from Eq. (3) can be derived as:

$$v = \left( 16.50 \left( \frac{E_0}{S_0} \right) - 1.33 \right) \times S_0 \exp \left\{ -2.447 \ln \left[ 1 + \left( 1332.21 \frac{E_0}{S_0} - 1.74 \right) t^2 \right] \right\} \quad (11)$$

Our previous research obtained that the best ratio to tenderize GP to make fishery products with improved texture was 0.40%

**Table 1—Fitting values of kinetic parameters *a* and *b* from Eq. (5) with different  $E_0/S_0$  ratios under 0 °C, pH 6.8.<sup>a</sup>**

| $S_0$ | $E_0$ | $E_0/S_0$ (%) | <i>a</i> (min <sup>-1</sup> ) | <i>b</i>       | <i>a<sub>m</sub></i> (min <sup>-1</sup> ) |
|-------|-------|---------------|-------------------------------|----------------|---|
| 1.55  | 15.00 | 0.97          | 15.58 ± 2.84a                 | 0.25 ± 0.05A   | 45.74 ± 17.75b                            |
| 1.55  | 7.50  | 0.48          | 9.96 ± 2.62a                  | 0.32 ± 0.03AB  | 6.71 ± 1.32a                              |
| 1.55  | 11.00 | 0.71          | 9.50 ± 3.31a                  | 0.38 ± 0.08ABC | 10.89 ± 2.67a                             |
| 1.55  | 3.75  | 0.24          | 2.00 ± 0.70a                  | 0.41 ± 0.08ABC | 2.32 ± 0.26a                              |
| 3.50  | 15.00 | 0.43          | 5.80 ± 0.81a                  | 0.48 ± 0.11ABC | 4.91 ± 0.17a                              |
| 3.50  | 7.50  | 0.21          | 1.89 ± 0.46a                  | 0.43 ± 0.09BC  | 2.01 ± 0.15a                              |
| 3.50  | 3.75  | 0.11          | 0.93 ± 0.17a                  | 0.55 ± 0.19CD  | 0.71 ± 0.09a                              |
| 7.50  | 15.00 | 0.20          | 3.02 ± 1.12a                  | 0.52 ± 0.14CD  | 2.26 ± 0.22a                              |
| 7.50  | 7.50  | 0.10          | 1.02 ± 0.43a                  | 0.68 ± 0.8CD   | 0.59 ± 0.04a                              |
| 7.50  | 3.75  | 0.05          | 0.85 ± 0.30a                  | 0.86 ± 0.10E   | —   |

<sup>a</sup>  $S_0$  (mg/mL),  $E_0$  ( $\times 10^{-3}$  mg/mL),  $E_0/S_0$  (%). Values are presented as mean  $\pm$  SD ( $n = 3$ ). Values with different lowercase inline letters in each row of the same  $E_0/S_0$  and values with different uppercase letters in the column of *b* values indicate significant differences by the Duncan's multiple range test ( $p < .05$ ).

( $E_0/S_0$ ), which fell in the range (0.10% to 0.71%) of this kinetic model. Further investigation, such as protein compositional and nanostructural changes, FAA generation of 0.40% ( $E_0/S_0$ ) group, will help to elaborate the enzyme mechanism.

### SDS-PAGE quantification

The example of SDS PAGE images is shown in Figure. 2, and the quantification result is shown in Table 2. It was obvious that myosin heavy chain (MHC) was degraded dramatically from 22.88% before bromelain treatment to 12.03% after 2 min enzyme reaction. After 2 min, the band intensity of MHC remained stable, indicating there was no degradation of MHC afterwards. Myosin is the major component of myofibril and determines the gel property of meat product. The significant activity of bromelain towards MHC demonstrated the significantly tenderizing effect on the GP and other meat (Ha, Bekhit, Carne, & Hopkins, 2012).

It can also be observed that proteins ranging from 60 to 90 kDa were generated after bromelain treatment, which were myosin subfragments (Liu, True, & Xiong, 2015; Rawdkuen, Sai-Ut, Khansorn, Chaijan, & Benjakul, 2009). The band intensity of those myosin subfragments remained stable after 2 min hydrolysis, which was consistent with the changes of MHC. The band intensity of Troponin T (29 kDa) decreased after 6 min hydrolysis, indicating the mild proteolytic effect towards Troponin T, which agreed well with previous findings (Rawdkuen et al., 2009). Troponin T is associated with the regulation of muscle contraction (Delbarre-Ladrat et al., 2006), and its degradation contributes to the meat tenderization. The parvalbumin (12 kDa) was degraded in the first 8 min and maintained its intensity at 2.44% from 10 min onwards. For other subunits of myofibril, bromelain didn't exhibit enzymatic activity towards them, such as actin (42 kDa), trypomyosin (35 kDa), myosin light chains (MLC; 16 to 25 kDa), troponin C (15 kDa) and undefined band fragments (33 kDa and 49 kDa; Kim & Taub, 1991).

### FAA analysis

The FAAs of three representative samples after 0, 8, and 20 min hydrolysis were analyzed by HPLC-MS/MS. Table 3 shows the detailed information of the detected FAAs, although Table 4 shows the quantification results of the FAAs. It was obvious that FAAs increased after enzymatic treatment, and  $\beta$ -alanine, leucine and sarcosine were generated.  $\beta$ -Alanine is an intrinsic amino acid in marine species, and is a precursor for carnosine and L-histidine.  $\beta$ -Alanine also contributes to improve the muscle structure (Culbertson, Kreider, Greenwood, & Cooke, 2010). Leucine is one of the essential amino acids, although sarcosine is one of the extracts

from fish muscle with low concentration (Raksakulthai, Lee, & Haard, 1986).

The concentration of FAAs were calculated based on the internal standard. Through comparing the peak areas of  $\beta$ -alanine, leucine, sarcosine, and phenylalanine with the external standard, the concentration of  $\beta$ -alanine, leucine, sarcosine, and phenylalanine is lower than 0.02 mM, which is beyond the range of the standard curve. Therefore, only glycine, alanine, lysine, glutamic acid, ornithine, and methionine sulfoxide were quantified through external amino acids standards.

Table 4 showed that there was a general increase of glycine, alanine, lysine, glutamic acid, ornithine, and methionine sulfoxide during the hydrolysis process, indicating the increased DH. It was consistent with previous finding that bromelain cleaved peptide bonds at the carbonyl end of lysine, alanine, and glycine (Godfrey & Reichelt, 1983). It was also reported that the flavoring agent hydrolyzed from shrimp processing byproducts by bromelain had increased glutamic acid, glycine and alanine, which was comparable with our results (Cheung & Li-Chan, 2014).

Lysine had the highest initial concentration of 0.167 mmol/L and it increased to 0.226 and 0.317 mmol/L, respectively, after 8 and 20 min of hydrolysis. Glycine showed gradual increase from 0.143 mmol/L before hydrolysis to 0.170 and 0.201 mmol/L after 8 and 20 min hydrolysis, respectively. The abundant lysine and glycine in fish and the bromelain preferred cleavage site explained the abundance of lysine and glycine in the hydrolysate (Iwasaki & Harada, 1985). The initial concentration of glutamic acid was 0.098 mmol/L, which was lower compared with lysine and glycine, and it increased to 0.148 and 0.227 mmol/L after 8 and 20 min hydrolysis. Methionine sulfoxide is also detected through LC-MS/MS with the lowest concentration throughout the hydrolysis process. The presence of methionine sulfoxide indicates the oxidation of the sulfur of methionine before and after hydrolysis (Hoar & Randall, 1972). Interestingly, other essential amino acids such as arginine, histidine, cysteine, and proline were not detected, indicating the active cleavage site of bromelain is not at those amino acids.

In general, the concentration of glycine, alanine, lysine, methionine sulfoxide, ornithine and glutamic acid increased by 0.058, 0.039, 0.150, 0.040, 0.056, and 0.129 mmol/L, respectively, indicating that the preferential cleavage sites of bromelain were in the descending order of lysine, glutamic acid, glycine, ornithine, methionine sulfoxide, and alanine. Glutamic acid, glycine, and alanine are flavorful, providing palatable and sweetish taste, which would improve the acceptance of fishery products made from GP (Bu, Dai, Zhou, Lu, & Jiang, 2013).

Table 2—Effects of hydrolysis time on the band intensity ( $\geq 0.005\%$ ) of myofibril proteins from SDS-PAGE results.<sup>a</sup>

| $M_w$ (kDa) | Percentage band volume (% total band volume) |               |               |               |               |               |               |               |                      |  |  | Protein |
|-------------|--|---------------|---------------|---------------|---------------|---------------|---------------|---------------|----------------------|--|--|---------|
|             | Hydrolysis time (min)                        |               |               |               |               |               |               |               |                      |  |  |         |
|             | 0  | 2             | 4             | 6             | 8             | 10            | 12            | 15            |                      |  |  |         |
| 205 – 220   | 22.88 ± 6.30b                                | 12.03 ± 3.62a | 9.69 ± 1.52a  | 11.26 ± 3.46a | 11.15 ± 2.65a | 9.39 ± 1.96a  | 9.30 ± 3.37a  | 9.03 ± 3.48a  | Myosin heavy chain   |  |  |         |
| 90          | 0.76 ± 0.17a                                 | 3.24 ± 0.71b  | 3.75 ± 1.32b  | 2.90 ± 0.40b  | 2.96 ± 1.16b  | 2.88 ± 0.08b  | 2.71 ± 0.46b  | 2.69 ± 0.20b  | Myosin subfragment-1 |  |  |         |
| 75          | 1.34 ± 0.10a                                 | 7.28 ± 0.35b  | 7.40 ± 1.32b  | 6.72 ± 0.17b  | 6.55 ± 0.76b  | 6.80 ± 1.12b  | 6.63 ± 0.30b  | 6.78 ± 1.37b  | Myosin subfragment-2 |  |  |         |
| 60          | 1.04 ± 0.19a                                 | 2.68 ± 1.00b  | 2.86 ± 0.37b  | 2.47 ± 0.76b  | 2.52 ± 0.67b  | 3.11 ± 0.42b  | 2.54 ± 0.47b  | 2.86 ± 0.82b  | Myosin subfragment-3 |  |  |         |
| 49          | 4.56 ± 0.80a                                 | 3.89 ± 0.71a  | 3.69 ± 1.25a  | 3.09 ± 0.96a  | 3.06 ± 1.14a  | 3.79 ± 0.69a  | 3.41 ± 0.87a  | 2.95 ± 0.83a  | –                    |  |  |         |
| 42          | 7.31 ± 0.76a                                 | 8.39 ± 0.87a  | 8.52 ± 0.47a  | 8.44 ± 2.13a  | 8.84 ± 1.87a  | 8.60 ± 0.92a  | 8.27 ± 1.82a  | 9.09 ± 1.18a  | Actin                |  |  |         |
| 35          | 21.17 ± 2.84a                                | 21.85 ± 0.38a | 23.99 ± 5.89a | 26.01 ± 3.32a | 24.32 ± 1.32a | 25.85 ± 4.65a | 27.35 ± 4.92a | 23.85 ± 1.25a | Tropomyosin          |  |  |         |
| 33          | 3.00 ± 1.32a                                 | 3.95 ± 0.79a  | 4.14 ± 0.57a  | 4.34 ± 1.17a  | 4.98 ± 0.32a  | 4.44 ± 0.27a  | 4.70 ± 0.81a  | 4.56 ± 0.77a  | –                    |  |  |         |
| 29          | 2.43b  | 2.26b         | 2.59b         | 1.36a         | 1.38a         | 1.88ab        | 1.31a         | 1.98ab        | Troponin – T         |  |  |         |
| 16 – 25     | 27.23 ± 5.11a                                | 26.24 ± 1.94a | 27.16 ± 4.31a | 26.81 ± 3.28a | 26.56 ± 4.24a | 26.42 ± 2.84a | 27.33 ± 2.82a | 27.12 ± 0.92a | Myosin light chains  |  |  |         |
| 15          | 9.92 ± 2.60a                                 | 10.57 ± 2.91a | 10.91 ± 3.04a | 10.93 ± 3.41a | 10.63 ± 3.44a | 10.65 ± 3.52a | 11.29 ± 3.32a | 10.86 ± 0.92a | Troponin C           |  |  |         |
| 12          | 4.16 ± 0.95c                                 | 4.33 ± 0.77c  | 3.50 ± 0.69b  | 3.57 ± 0.83b  | 2.94 ± 0.66ab | 2.44 ± 0.41a  | 2.42 ± 0.30a  | 2.42 ± 0.34a  | Parvalbumin          |  |  |         |

<sup>a</sup>Sample with 0.40%  $E_0/S_0$  ratio (%). Values are presented as mean ± SD ( $n = 3$ ). Values with different lowercase inline letters in each row of same  $M_w$  indicate significant differences among different hydrolysis time by the Duncan's multiple range test ( $p < .05$ ).

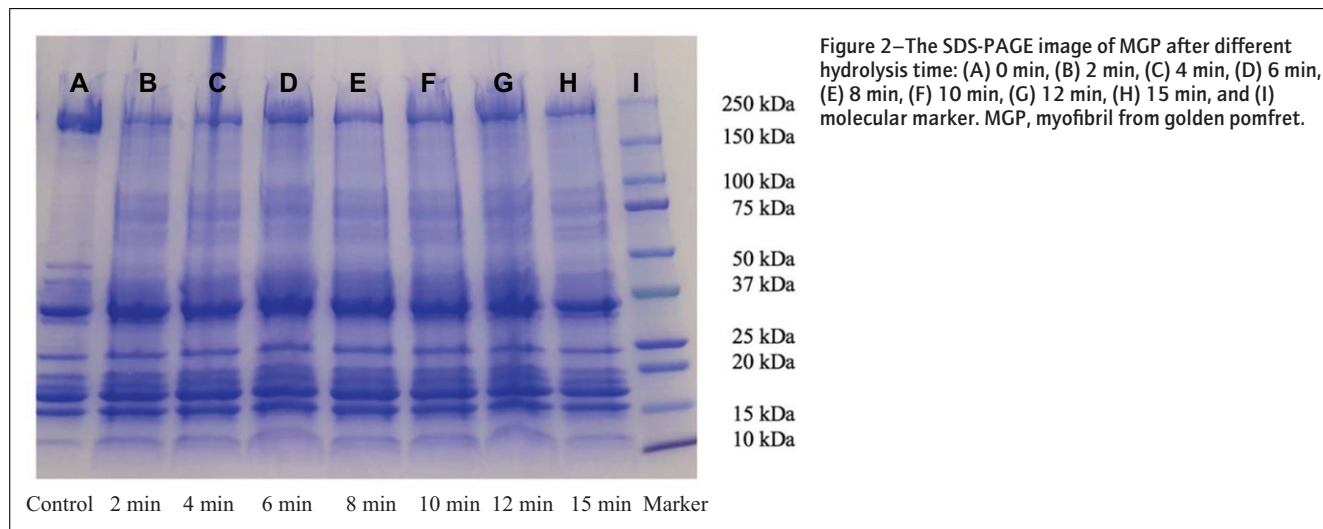


Figure 2—The SDS-PAGE image of MGP after different hydrolysis time: (A) 0 min, (B) 2 min, (C) 4 min, (D) 6 min, (E) 8 min, (F) 10 min, (G) 12 min, (H) 15 min, and (I) molecular marker. MGP, myofibril from golden pomfret.

Table 3—Free amino acids detected by HPLC-MS/MS.<sup>a</sup>

| Retention time (min) | Reaction time (min) |   |    | Derivative ( $M_w + 1$ ) | FAA                        | MS/MS ( $M_w$ ) |
|----------------------|---------------------|---|----|--------------------------|----------------------------|-----------------|
|                      | 0                   | 8 | 20 |                          |                            |                 |
| 5.7                  | ✓                   | ✓ | ✓  | 317                      | Homoarginine <sup>IS</sup> | 84, 128, 170    |
| 6.9                  | ✓                   | ✓ | ✓  | 294                      | Methionine sulfoxide       | 234, 142        |
| 7.2                  |                     | ✓ | ✓  | 318                      | Beta-Alanine               | 98, 116, 158    |
| 8.1                  |                     | ✓ | ✓  | 260                      | Leucine                    | 172             |
| 8.6                  | ✓                   | ✓ | ✓  | 204                      | Glycine                    | 144, 118, 162   |
| 10.6                 | ✓                   | ✓ | ✓  | 218                      | Alanine                    | 130, 158, 88    |
| 12.8                 | ✓                   | ✓ | ✓  | 347                      | Ornithine                  | 287, 156, 227   |
| 12.9                 | ✓                   | ✓ | ✓  | 361                      | Lysine                     | 301, 170        |
| 13.5                 |                     | ✓ | ✓  | 218                      | Sarcosine                  | 158, 88         |
| 15.3                 | ✓                   | ✓ | ✓  | 318                      | Glutamic acid              | 172, 258, 230   |
| 17.5                 | ✓                   | ✓ | ✓  | 294                      | Phenylalanine              | 206, 120        |

<sup>a</sup>Presence of the amino acids was indicated by a “✓”. The internal standard homoarginine was indicated with superscript letters “IS”.

Table 4—Effects of hydrolysis time on the composition of free amino acids by HPLC-MS/MS.<sup>a</sup>

| Amino acid concentration ( $10^{-1}$ mM) | Reaction time (min) |              |              |
|--|---------------------|--------------|--------------|
|  | 0                   | 8            | 20           |
| Glycine                                  | 1.43 ± 0.10a        | 1.70 ± 0.12b | 2.01 ± 0.11c |
| Alanine                                  | 0.71 ± 0.06a        | 0.83 ± 0.07b | 1.10 ± 0.09c |
| Lysine                                   | 1.67 ± 0.10a        | 2.26 ± 0.12b | 3.17 ± 0.13c |
| Glutamic acid                            | 0.98 ± 0.07a        | 1.48 ± 0.09b | 2.27 ± 0.10c |
| Ornithine                                | 0.49 ± 0.03a        | 0.60 ± 0.04b | 1.05 ± 0.05c |
| Methionine sulfoxide                     | 0.37 ± 0.02a        | 0.40 ± 0.03b | 0.77 ± 0.03c |

<sup>a</sup>Sample with 0.40%  $E_0/S_0$  ratio. Values are presented as mean ± SD ( $n = 3$ ). Values with different lowercase inline letters at the same row indicate significant differences by the Duncan's multiple range test ( $p < .05$ ).

### Nanostructure changes of MGP

Figure 3 shows the AFM images of myofibril after different hydrolysis time. Myofibril remained intact strip-like structure before hydrolysis (Feng, Ng, Mikš-Krajnik, & Yang, 2017b; Kong, Tang, Lin, & Rasco, 2008). Table 5 showed that the length of myofibril before hydrolysis was greater than 15  $\mu\text{m}$ , and the width and height was 5.05 and 0.51  $\mu\text{m}$ , respectively. After bromelain treatment, myofibril remained strip-like structure; however, there was significant degradation as shown in Figure 3. The length and width of myofibril decreased to 10.79 and 4.68  $\mu\text{m}$  after 4 min hydrolysis, indicating the hydrolytic effect of bromelain on my-

ofibril. In Figure 3B, the breaking of the sarcomere was observed as indicated by the red arrow. However, there was no significant difference between the height of control and 4 min hydrolysis samples, indicating that the bromelain hydrolyzed myofibrils from the dimension of length and width.

The changes of length are mainly due to the breakage of the sarcomeres, as bromelain may hydrolyze Z-lines between each sarcomere, leading to myofibril fragmentation (Feng et al., 2017b). The changes of the width were caused by the separation of myofibril bundles as shown in Figure 3. Myofibril is basically composed of thick and thin filaments, whereas the thick and thin filaments

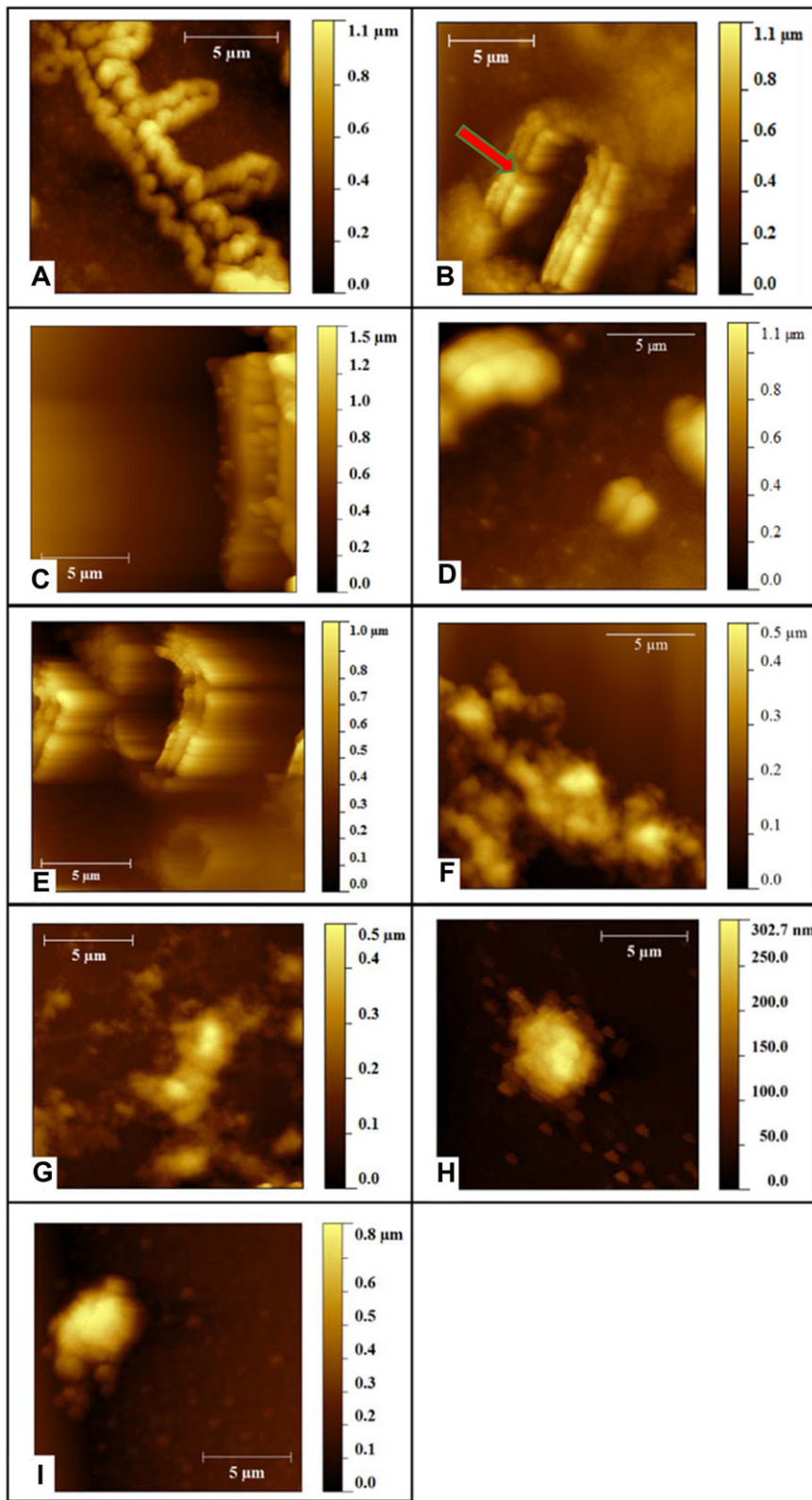


Figure 3–AFM images of MGP treated with bromelain after different time: (A) 0 min, (B) 4 min, (C) 6 min, (D) 8 min, (E) 10 min, (F) 12 min, (G) 15 min, (H) 20 min, and (I) 30 min. MGP, myofibril from golden pomfret.

are composed of myosin and actin, respectively. Trypomycin and troponin are the proteins crosslink myosin and actin filaments to start and stop and the muscle contraction, whereas troponin is composed of troponin T, troponin C, and troponin I (Ertbjerg & Puolanne, 2017). From the SDS PAGE results, bromelain has

no hydrolytic effects towards trypomycin, troponin C, and troponin I, whereas only exerted mild hydrolytic effect to Troponin T. Therefore, bromelain is not able to separate the thick and thin filaments of myofibrils to decrease the height of myofibrils. Similar findings can also be found in our previous published paper (Feng



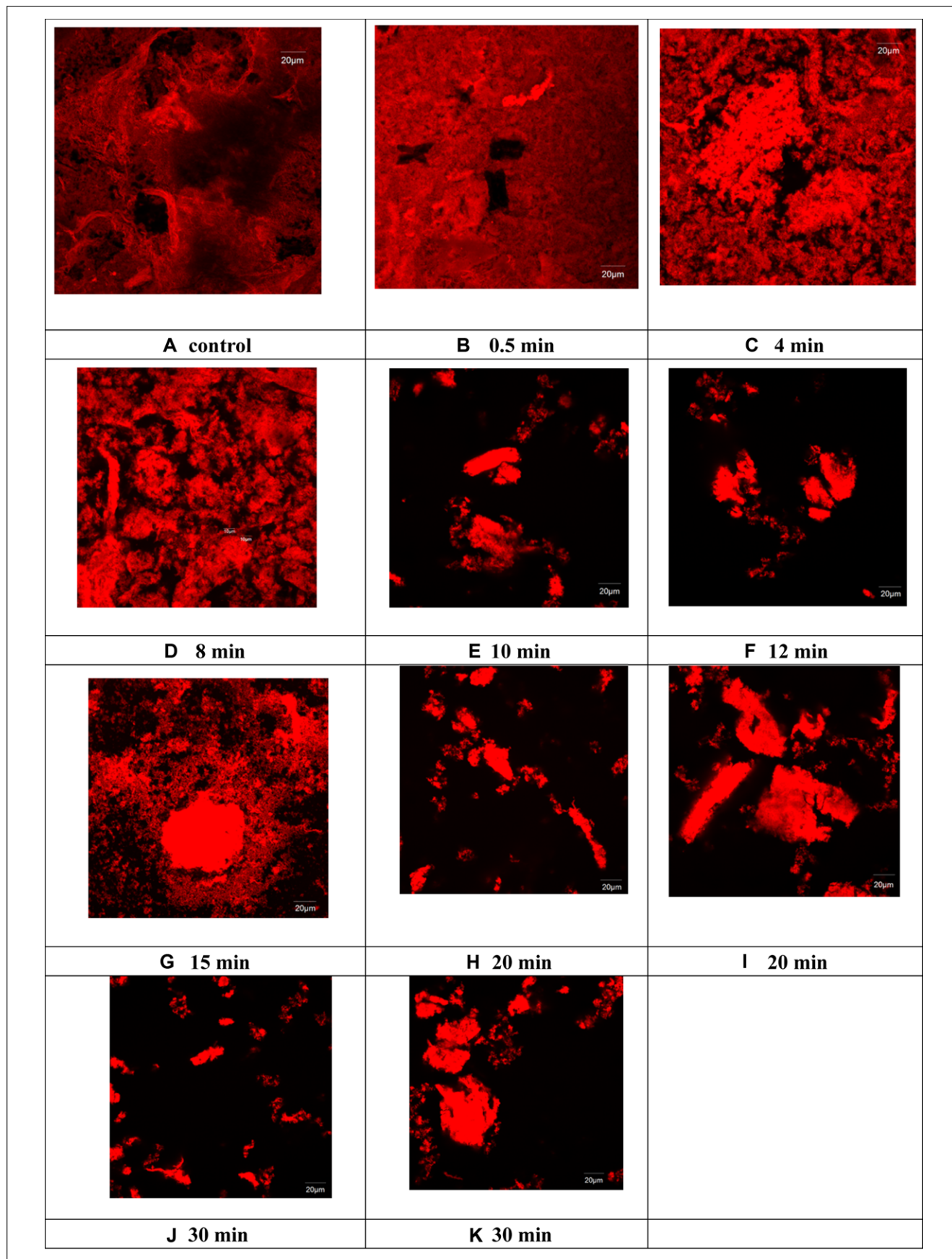


Figure 4—CLSM images of MGP treated with bromelain after different time: (A) 0 min, (B) 0.5 min, (C) 4 min, (D) 8 min, (E) 10 min, (F) 12 min, (G) 15 min, (H, I) 20 min, and (J, K) 30 min. CLSM, confocal laser scanning microscopy; MGP, myofibril from golden pomfret.

**Table 5—Effects of hydrolysis time on the dimensions of myofibrils.<sup>a</sup>**

| Dimension                | Time (min)       |                   |                  |                    |                     |                     |                    |
|--------------------------|------------------|-------------------|------------------|--------------------|---------------------|---------------------|--------------------|
|                          | 0                | 4                 | 8                | 12                 | 15                  | 20                  | 30                 |
| Length ( $\mu\text{m}$ ) | >15a             | 10.79 $\pm$ 1.32b | 5.14 $\pm$ 0.82c | 5.03 $\pm$ 0.61c   | 4.82 $\pm$ 1.30c    | 3.66 $\pm$ 0.74c    | 3.16 $\pm$ 0.71c   |
| Width ( $\mu\text{m}$ )  | 5.05 $\pm$ 0.11a | 4.68 $\pm$ 1.42ab | 4.16 $\pm$ 1.42b | 3.79 $\pm$ 0.85b   | 3.34 $\pm$ 0.98c    | 3.10 $\pm$ 0.26c    | 3.15 $\pm$ 0.71c   |
| Height ( $\mu\text{m}$ ) | 0.51 $\pm$ 0.26a | 0.59 $\pm$ 0.14a  | 0.61 $\pm$ 0.08a | 0.48 $\pm$ 0.07a   | 0.24 $\pm$ 0.04b    | 0.23 $\pm$ 0.05b    | 0.19 $\pm$ 0.06b   |
| Area ( $\mu\text{m}$ )   | —                | —                 | —                | 772.5 $\pm$ 160.8c | 4000.1 $\pm$ 389.5a | 1267.7 $\pm$ 236.2b | 415.9 $\pm$ 149.8d |

The length, width, and height of myofibrils were analyzed using the line profile extraction function of Gwyddion software (AFM Workshop, Signal Hill, Calif, U.S.A.).

‘—’ indicates that the protein aggregates are not detected.

<sup>a</sup>Sample with 0.40%  $E_0/S_0$  ratio (%). Values are presented as mean  $\pm$  SD ( $n = 15$ ). Values with different lowercase inline letters at the same dimension indicate significant differences by the Duncan's multiple range test ( $p < .05$ ).

et al., 2016) that the endogenous enzyme and bacteria degraded myofibril mainly from the dimension of length and width instead of height.

After 8 min hydrolysis, no significant decrease of myofibril length was observed, and there were no significant differences detected for the myofibril width and height as well. From 12 min onwards, the strip-like myofibril structure was no longer observed, whereas the granulation and aggregation of myofibril hydrolysis product was observed through AFM, which might be due to the protein self-assembly (Basu, Li, & Leong, 2011; Dong et al., 2016). Figure 4 shows the selected CLSM images during bromelain hydrolysis. Before hydrolysis, the control images showed clear intact fibers that resembled the rod-like structures shown in the AFM images. In the sample that was hydrolyzed for 10 min, the length of myofibrils decreased, similar as that revealed by AFM. Aggregates were formed after the myofibrils were hydrolyzed for 12 min, corresponding well to the AFM results. The area of the aggregates was measured, and no specific trend was discovered in Table 5. After bromelain hydrolysis, the protein structure denatured and unfolded, and self-assembled to amorphous aggregates (Basu et al., 2011; Dong et al., 2016).

## Conclusion

In this study, an enzyme kinetic model was built as:  $x = 2.447 \times \ln[1 + (1332.21 \times \frac{E_0}{S_0} - 1.74)t]$ , which indicated the dependency of DH on  $E_0$ ,  $S_0$ , and  $t$ . The hydrolysis rate was calculated from:

$$v = \left( 16.50 \frac{E_0}{S_0} - 1.33 \right) \times S_0 \exp \left\{ -2.447 \ln \left[ 1 + \left( 1332.21 \frac{E_0}{S_0} - 1.74 \right) t^2 \right] \right\}.$$

BML exerted great hydrolytic effect on MHC while mild hydrolytic effect on troponin *T*. Interestingly, BML did not have hydrolytic effects on actin (42 kDa), tryptomyosin (35 kDa), MLC (16 to -25 kDa), and troponin C (15 kDa). A general increase of FAA was observed during the hydrolysis, which was consistent with the increased DH. Furthermore, cleavage preferences of bromelain were revealed to deepen the understanding of the enzyme mechanism that the preferential cleavage sites of bromelain were in the descending order of lysine, glutamic acid, glycine, ornithine, methionine sulfoxide, and alanine. AFM results showed that the rod-like myofibrils with length longer than 15  $\mu\text{m}$  before hydrolysis were degraded to 5.14  $\mu\text{m}$  after 8 min BML treatment, and the granulation of protein hydrolysates was observed after 12 min hydrolysis, which agreed well with the confocal results. The kinetic and mechanism studies of BML hydrolysis effect on MGP have potential applications in fishery processing. As DH is related to the meat tenderness, kinetic models can be applied to

predict the time and enzyme concentration needed to tenderize meat to desired texture.

## Acknowledgments

The authors acknowledge the financial support by the Singapore Ministry of Education Academic Research Fund Tier 1 (R-143-000-583-112). Projects 31371851 and 31471605 supported by NSFC and an industry project from Fujian Putian Sea-100 Food Co., Ltd. (R-143-000-633-597) also contributed to this research.

## Authors' Contributions

Xiao Feng designed this study, interpreted, the results and drafted the manuscript. Shasha Hang did part of the experiment and analyzed the data. Yige Zhou contributed to the protein composition analysis, whereas Qin Liu contributed to the data analysis. Dr. Hongshun Yang supervised the project and revised the manuscript.

## References

- Ahern, T. J., & Klibanov, A. M. (1985). The mechanism of irreversible enzyme inactivation at 100 degrees C. *Science*, 228, 1280–1285. <https://doi.org/10.1126/science.4001942>
- Himonides A. T., Taylor A. K. D., & Morris A. J. (2011). A study of the enzymatic hydrolysis of fish frames using model systems. *Food and Nutrition Sciences*, 2, 575–585. <https://doi.org/10.4236/fns.2011.26081>
- Arshad, Z. I. M., Amid, A., Yusof, F., Jaswir, I., Ahmad, K., & Loke, S. P. (2014). Bromelain: An overview of industrial application and purification strategies. *Applied Microbiology and Biotechnology*, 98, 7283–7297. <https://doi.org/10.1007/s00253-014-5889-y>
- Basu, A., Li, X., & Leong, S. S. J. (2011). Refolding of proteins from inclusion bodies: Rational design and recipes. *Applied Microbiology and Biotechnology*, 92, 241–251. <https://doi.org/10.1007/s00253-011-3513-y>
- Bradford, M. M. (1976). A rapid and sensitive method for the quantitation of microgram quantities of protein utilizing the principle of protein-dye binding. *Analytical Biochemistry*, 72, 248–254. [https://doi.org/10.1016/0003-2697\(76\)90527-3](https://doi.org/10.1016/0003-2697(76)90527-3)
- Bu, J., Dai, Z., Zhou, T., Lu, Y., & Jiang, Q. (2013). Chemical composition and flavor characteristics of a liquid extract occurring as waste in crab (*Ovalipes punctatus*) processing. *Journal of the Science of Food and Agriculture*, 93, 2267–2275. <https://doi.org/10.1002/jsfa.6036>
- Cheung, I. W., & Li-Chan, E. C. (2014). Application of taste sensing system for characterization of enzymatic hydrolysates from shrimp processing by-products. *Food Chemistry*, 145, 1076–1085. <https://doi.org/10.1016/j.foodchem.2013.09.004>
- Culbertson, J. Y., Kreider, R. B., Greenwood, M., & Cooke, M. (2010). Effects of beta-alanine on muscle carnosine and exercise performance: a review of the current literature. *Nutrients*, 2, 75–98. <https://doi.org/10.3390/nu2010075>
- Delbarre-Ladrat, C., Chéret, R., Taylor, R., & Verrez-Bagnis, V. (2006). Trends in postmortem aging in fish: Understanding of proteolysis and disorganization of the myofibrillar structure. *Critical Reviews in Food Science and Nutrition*, 46, 409–421. <https://doi.org/10.1080/10408390591000929>
- Delles, R. M., Xiong, Y. L., & True, A. D. (2011). Mild protein oxidation enhanced hydration and myofibril swelling capacity of fresh ground pork muscle packaged in high oxygen atmosphere. *Journal of Food Science*, 76, C760–C767. <https://doi.org/10.1111/j.1750-3841.2011.02195.x>
- Dong, F., Dong, X., Zhou, L., Xiao, H., Ho, P. Y., Wong, M. S., & Wang, Y. (2016). Doxorubicin-loaded biodegradable self-assembled zein nanoparticle and its anti-cancer effect: Preparation, in vitro evaluation, and cellular uptake. *Colloids and Surfaces B: Biointerfaces*, 140, 324–331. <https://doi.org/10.1016/j.colsurfb.2015.12.048>
- Ertbjerg, P., & Puolanne, E. (2017). Muscle structure, sarcomere length and influences on meat quality: a review. *Meat Science*, 132, 139–152.
- Esti, M., Benucci, I., Liburdi, K., & Garzillo, A. M. V. (2015). Immobilized pineapple stem bromelain activity in a wine-like medium: Effect of inhibitors. *Food and Bioprocess Technology*, 9, 84–89. <https://doi.org/10.1016/j.fbp.2013.12.001>
- Feng, X., Bansal, N., & Yang, H. (2016). Fish gelatin combined with chitosan coating inhibits myofibril degradation of golden pomfret (*Trachinotus blochii*) fillet during cold storage. *Food Chemistry*, 200, 283–292. <https://doi.org/10.1016/j.foodchem.2016.01.030>
- Feng, X., Fu, C., & Yang, H. (2017a). Gelatin addition improves the nutrient retention, texture, and mass transfer of fish balls without altering their nanostructure during boiling. *LWT—Food Science and Technology*, 77, 142–151. <https://doi.org/10.1016/j.lwt.2016.11.024>

- Feng, X., Ng, V. K., Mikš-Krajnik, M., & Yang, H. (2017b). Effects of fish gelatin and tea polyphenol coating on the spoilage and degradation of myofibril in fish fillet during cold storage. *Food and Bioprocess Technology*, *10*, 89–102. <https://doi.org/10.1007/s11947-016-1798-7>
- Feng, X., Zhu, Y., Liu, Q., & Yang, H. (2017c). Effects of bromelain tenderization on texture, myofibrillar protein, and flavor of fish balls. *Food and Bioprocess Technology*, *10*, 1918–1930. <https://doi.org/10.1007/s11947-017-1963-7>
- Gbogouri, G., Linder, M., Fanni, J., & Parmentier, M. (2004). Influence of hydrolysis degree on the functional properties of salmon byproducts hydrolysates. *Journal of Food Science*, *69*, C615–C622. <https://doi.org/10.1111/j.1365-2621.2004.tb09909.x>
- Gerelt, B., Ikeuchi, Y., & Suzuki, A. (2000). Meat tenderization by proteolytic enzymes after osmotic dehydration. *Meat Science*, *56*, 311–318. [https://doi.org/10.1016/S0309-1740\(00\)00060-7](https://doi.org/10.1016/S0309-1740(00)00060-7)
- Godfrey, T., & Reichelt, J. (1983). *Introduction to industrial enzymology*. London, UK: Macmillan Press.
- González-Tello, P., Camacho, F., Jurado, E., Paez, M., & Guadix, E. (1994). Enzymatic hydrolysis of whey proteins: I. Kinetic models. *Biotechnology and Bioengineering*, *44*, 523–528. <https://doi.org/10.1002/bit.260440415>
- Ha, M., Bekhit, A. E.-D. A., Carne, A., & Hopkins, D. L. (2012). Characterization of commercial papain, bromelain, actinidin, and zingibain protease preparations and their activities toward meat proteins. *Food Chemistry*, *134*, 95–105. <https://doi.org/10.1016/j.foodchem.2012.02.071>
- Iwasaki, M., & Harada, R. (1985). Proximate and amino acid composition of the roe and muscle of selected marine species. *Journal of Food Science*, *50*, 1585–1587. <https://doi.org/10.1111/j.1365-2621.1985.tb10539.x>
- Kim, H. K., Ha, S. J., Kim, Y. H., Kim, Y. U., Song, K. M., Lee, N. H., & Jung, S. K. (2017). Protein extraction from porcine myocardium using ultrasonication. *Journal of Food Science*, *82*, 1059–1065. <https://doi.org/10.1111/1750-3841.13694>
- Kim, H. J., & Taub, I. A. (1991). Specific degradation of myosin in meat by bromelain. *Food Chemistry*, *40*, 337–343. [https://doi.org/10.1016/0308-8146\(91\)90117-7](https://doi.org/10.1016/0308-8146(91)90117-7)
- Kirk, O., Borchert, T. V., & Fuglsang, C. C. (2002). Industrial enzyme applications. *Current Opinion in Biotechnology*, *13*, 345–351. [https://doi.org/10.1016/S0958-1669\(02\)00328-2](https://doi.org/10.1016/S0958-1669(02)00328-2)
- Klompong, V., Benjakul, S., Kantachote, D., & Shahidi, F. (2007). Antioxidative activity and functional properties of protein hydrolysate of yellow stripe trevally (*Selaroides leptolepis*) as influenced by the degree of hydrolysis and enzyme type. *Food Chemistry*, *102*, 1317–1327. <https://doi.org/10.1016/j.foodchem.2006.07.016>
- Kong, F., Tang, J., Lin, M., & Rasco, B. (2008). Thermal effects on chicken and salmon muscles: Tenderness, cook loss, area shrinkage, collagen solubility, and microstructure. *LWT-Food Science and Technology*, *41*, 1210–1222. <https://doi.org/10.1016/j.lwt.2007.07.020>
- Liu, Z., True, A. D., & Xiong, Y. L. (2015). Curtailing oxidation-induced loss of myosin gelling potential by pyrophosphate through shielding the S1 subfragment. *Journal of Food Science*, *80*, C1468–C1475. <https://doi.org/10.1111/1750-3841.12904>
- Liu, C., & Xiong, Y. L. (2015). Oxidation-initiated myosin subfragment cross-linking and structural instability differences between white and red muscle fiber types. *Journal of Food Science*, *80*, C288–C297. <https://doi.org/10.1111/1750-3841.12749>
- Lobo, F., Ventanas, S., Morcuende, D., & Estévez, M. (2016). Underlying chemical mechanisms of the contradictory effects of NaCl reduction on the redox-state of meat proteins in fermented sausages. *LWT - Food Science and Technology*, *69*, 110–116. <https://doi.org/10.1016/j.lwt.2016.01.04>
- Loneragan, E. H., Zhang, W., & Loneragan, S. M. (2010). Biochemistry of postmortem muscle—Lessons on mechanisms of meat tenderization. *Meat Science*, *86*, 184–195. <https://doi.org/10.1016/j.meatsci.2010.05.004>
- Maresca, P., & Ferrari, G. (2017). Modelling of the kinetics of Bovine Serum Albumin enzymatic hydrolysis assisted by high hydrostatic pressure. *Food and Bioprocess Technology*, *105*, 1–11. <https://doi.org/10.1016/j.fbp.2017.03.006>
- Mohtar, N. F., Perera, C., & Quek, S. Y. (2010). Optimization of gelatine extraction from hoki (*Macrurus novaezelandiae*) skins and measurement of gel strength and SDS-PAGE. *Food Chemistry*, *122*, 307–313. <https://doi.org/10.1016/j.foodchem.2010.02.027>
- Raksakulthai, N., Lee, Y., & Haard, N. (1986). Effect of enzyme supplements on the production of fish sauce from male capelin (*Mallotus villosus*). *Canadian Institute of Food Science and Technology Journal*, *19*, 28–33. [https://doi.org/10.1016/S0315-5463\(86\)71377-1](https://doi.org/10.1016/S0315-5463(86)71377-1)
- Rawdkuen, S., Sai-Ut, S., Khamsorn, S., Chaijan, M., & Benjakul, S. (2009). Biochemical and gelling properties of tilapia surimi and protein recovered using an acid-alkaline process. *Food Chemistry*, *112*, 112–119. <https://doi.org/10.1016/j.foodchem.2008.05.047>
- Razzak, M. A., Kim, M., & Chung, D. (2016). Elucidation of aqueous interactions between fish gelatin and sodium alginate. *Carbohydrate Polymers*, *148*, 181–188. <https://doi.org/10.1016/j.carbpol.2016.04.035>
- Rebeca, B. D., Pena-Vera, M., & Diaz-Castaneda, M. (1991). Production of fish protein hydrolysates with bacterial proteases; yield and nutritional value. *Journal of Food Science*, *56*, 309–314. <https://doi.org/10.1111/j.1365-2621.1991.tb05268.x>
- Sasaoka, Y., Kishimura, H., Adachi, S., & Takagi, Y. (2017). Collagen peptides derived from the triple helical region of sturgeon collagen improve glucose tolerance in normal mice. *Journal of Food Biochemistry*, *42*. <https://doi.org/10.1111/jfbc.12478>
- Sow, L. C., & Yang, H. (2015). Effects of salt and sugar addition on the physico-chemical properties and nanostructure of fish gelatin. *Food Hydrocolloids*, *45*, 72–82. <https://doi.org/10.1016/j.foodhyd.2014.10.021>
- Suwal, S., Ketnawa, S., Huang, J. Y., & Liceaga, A. M. (2017). Electro-membrane fractionation of antioxidant peptides from protein hydrolysates of rainbow trout (*Oncorhynchus mykiss*) byproducts. *Innovative Food Science and Emerging Technologies*, *45*, 122–131. <https://doi.org/10.1016/j.ifset.2017.08.016>
- Thiansilakul, Y., Benjakul, S., & Shahidi, F. (2007). Compositions, functional properties and antioxidative activity of protein hydrolysates prepared from round scad (*Decapterus mamadsi*). *Food Chemistry*, *103*, 1385–1394. <https://doi.org/10.1016/j.foodchem.2006.10.055>
- Xu, W., Yu, G., Xue, C., Xue, Y., & Ren, Y. (2008). Biochemical changes associated with fast fermentation of squid processing by-products for low salt fish sauce. *Food Chemistry*, *107*, 1597–1604. <https://doi.org/10.1016/j.foodchem.2007.10.030>
- Zarei, M., Ghanbari, R., Tajabadi, N., Abdul-Hamid, A., Bakar, F. A., & Saari, N. (2016). Generation, fractionation, and characterization of iron-chelating protein hydrolysate from palm kernel cake proteins. *Journal of Food Science*, *81*, C341–C347. <https://doi.org/10.1111/1750-3841.13200>